Acta Materialia Transylvanica 8/2. (2025) 81–87.
DOI: Hungarian: https://doi.org/10.33923/amt-2025-02-07
English: https://doi.org/10.33924/amt-2025-02-07

Investigation of the Handheld Laser Welding Parameters

Balázs Ákos NAGY,[1] Kíra KOVÁCS,[2] Tünde Anna KOVÁCS[3]

[1] *Óbuda University, Bánki Donát Faculty of MEchanical and Safety Engineerig, Budapest, Hungary, nagy.balazs@bgk.uni-obuda.hu*

[2] *Óbuda University, Bánki Donát Faculty of MEchanical and Safety Engineerig, Budapest, Hungary, kira.kovacs3@gmail.com*

[3] *Óbuda University, Bánki Donát Faculty of MEchanical and Safety Engineerig, Budapest, Hungary, kovacs.tunde@bgk.uni-obuda.hu*

Abstract

High-performance handheld laser welding technologies have undergone significant advancements in recent years, particularly with the emergence of compact, cooled, and precise beam-shaping equipment. Handheld lasers (HL) possess all the advantages of their industrially applied, machine- or robotic-arm-guided counterparts. The key distinction lies in numerical beam control, which, alongside the parameters critical for successful welding, receives particular attention. This was due to the material- and penetration-depth-dependent program code table of the user-friendly Lightweld 1500 XT fiber laser welding equipment. During the experiments, S355 structural steel and DC01 cold-rolled steel sheets were welded in a T-joint configuration with varying sheet thicknesses, using identical material pairings. The used filler material was a Böhler EMK 8 Ø1 mm solid wire electrode, and the shielding gas was nitrogen with a 4.6. purity. We found that even with the settings recommended by the welding machine manufacturer, there were welding deviations, which suggests that the quality of manual welding also depends on the skill of the welder.

Keywords: *handheld laser welding, conduction laser welding, welding speed, filler material, nitride precipitations.*

1. Introduction

Fig. 1 shows the weld shapes typically created during laser welding.

Laser technologies are indispensable in our daily lives, particularly in industrial applications. This is especially true in welding technologies due to their precision, high power density, and relatively low thermal load on the base material **[1, 2, 3]**. Until recently, robust equipment has typically been used, referring to the excitation circuit and isolated workspaces. Thanks to advancements in fiber technology, excitation circuits can now be designed to match the size of industrial wire electrode (code: 13) or tungsten electrode (code: 14) shielded arc welding machines **[4]**. This has led to the development of handheld laser sources, which gained significant attention in the late 2000s (according to General Electronics Co.'s patent) **[4, 5]**. These first-generation laser sources did not yet possess the compact dimensions mentioned earlier, but current fourth-generation models, with advancements in cooling systems, have achieved this **[4, 6]**.

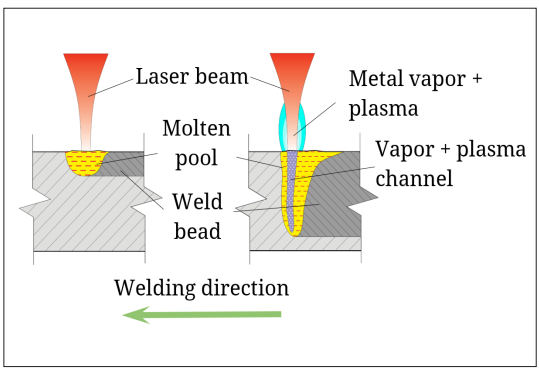

Fig. 1. *Difference between heat conduction (left) and deep-penetration (right) laser welding.*

The standard Welding and Allied Processes (MSZ ISO 4063: 2023) assigns identification codes to various processes, distinguishing between manual and automated variants of technologies operating on the same principles. Handheld laser welding lacks a specific designation but can be defined under code 521, which indicates high-energy-density (5), laser-based (2), and specifically solid-state (1) systems [7]. Key characteristics of this process include the use of Nd: YAG crystal ($Y_3Al_5O_{12}$/YAG: yttrium-aluminum-garnet doped with Nd^{3+} ions) as the typical laser medium, with an emission wavelength of 1064 nm (Near Infrared - NIR) [1, 2, 8]. Additionally, it operates in continuous wave (CW) mode, and due to variations in welding speed, it is limited to conduction welding during manual beam guidance.

At the end of the article, we evaluate the performance of the default programs of the IPG LightWeld 1500 XT laser equipment, courtesy of Intertechnika Ltd.

2. Parameters of Laser welding

To achieve a high-quality weld, it is essential to define and control the input parameters [3].]. The process begins with determining the weld geometry and the required material thickness, as these dictate the other adjustable parameters [9]. Parameters that can be controlled include the power setting on the equipment (potentially including beam oscillation), the gas flow rate on the shielding gas regulator, and the relative positioning of the workpieces using auxiliary tools (clamps, fixtures, welding table-template systems) or tack welding [3, 9]. Challenges with this process include maintaining a constant welding speed and ensuring the correct focus position and distance [6].

2.1. Laser Power

The laser output power (W, kW) determines the energy delivered to the base material, which influences the penetration depth [2].

Estimating the power requirement is common practice, as it depends on multiple factors. A simplified approach is based on energy density [10]:

$$I = \frac{P}{A} = \frac{4 \cdot P}{{d_{spot}}^2 \cdot \pi} \quad (1)$$

where:
I: energy density (W/cm^2),
P: laser power (W),
A: irradiated area (cm^2),
d_{spot}: spot diameter (cm).

The approach is applicable since we know the energy density range for conduction welding (10^4-10^6 W/cm^2); however, it must be noted that the formula neglects several factors. The following formula approximates based on the absorbed energy (Q_a; J) [1]:

$$\begin{aligned} Q_a &= Q_1 + Q_2 + Q_3 + Q_4 + Q_l = \\ &= m_a \cdot c_p \cdot \Delta T_m + m_a \cdot L_m + \\ &\quad + m_a \cdot c_p \cdot \Delta T_V + m_a \cdot L_V + Q_l \end{aligned} \quad (2)$$

where:
Q_1: energy required to heat the base material to its melting point,
Q_2: energy for melting, which requires latent heat,
Q_3: energy required to vaporize the molten material,
Q_4: energy demand for vaporization as a function of the latent heat of vaporization,
Q_l: energy lost through conduction, convection, evaporation, reflection, and radiation,
m_a: mass of the melted material (kg),
c_p : specific heat capacity (J/kg·K),
ΔT_m: temperature difference required for melting the base material (K),
L_m: latent heat of melting (J/kg),
ΔT_V: temperature difference required for the molten material to reach its boiling point (K),
L_V: latent heat of vaporization (J/kg).

Taking into account the volume (V) and density (ρ), the following formula is obtained **[1]**:

$$Q_a = \rho \cdot V \cdot \left(c_p \cdot \Delta T_m + L_m + c_p \cdot \Delta T_V + \cdot L_V\right) \quad (3)$$

With this, the absorbed energy has been determined. To obtain the power, it must be divided by the time required to melt the base material. If tack welding is not performed, the time can be determined using the formula:

$$t = \frac{\Delta x}{v} \quad (4)$$

where Δx is the melted length (mm), and v is the welding speed (mm/s). Accordingly, the power calculation is:

$$P = \frac{Q_a \cdot v}{\Delta x} \quad (5)$$

During manual beam guidance, the welding speed is difficult to determine and maintain at a constant value. Therefore, the approach based on the melting energy requirement is:

$$P = \rho \cdot \dot{V} \cdot \left(c_p \cdot \Delta T_m + L_m + c_p \cdot \Delta T_V + \cdot L_V\right) \quad (6)$$

where:

$\dot{V}$: the volume of molten material per unit time (m^3/s).

2.2. Welding Speed

Welding speed (feed rate) is one of the most critical process parameters during welding, as it directly affects the penetration depth, weld geometry, and the extent of the heat-affected zone (HAZ) [3, 9]. Increasing the speed reduces the specific heat input, resulting in a smaller molten pool and shallower penetration, while a lower speed leads to deeper penetration and a wider weld profile [3, 9].

The relationships discussed in the previous section were based on the Rosenthal equation, which can be rearranged to express the welding speed. Another approach is illustrated in Fig. 2, which outlines the interaction between three parameters: power (P), relative speed (v_r) and beam spot diameter (d_f) [11].

The ratios formed between these parameters yield physically meaningful and interpretable quantities. These ratios include power density (p; W/mm^2), specific heat input (q; W/mm), and the „residence time of a surface material point in the focus spot" (t_h; s) [11]. Power density indicates how concentrated the laser power is per unit area. Therefore, the denominator must be adjusted with a focus geometry factor (Y; –): for a square spot, Y = 1, while for a circular cross-section (more common), Y = π/4 (1). The specific heat input (line energy) reflects the heat energy delivered per 1 mm of length. This allows us to predict the outcome: at low P/vr, shallower penetration is observed, followed by faster cooling, resulting in a martensitic microstructure (in carbon steels), which increases the risk of cracking [10]. It is advisable to maintain this ratio at a higher value to achieve a proper weld. The interaction time is related to this: the longer energy is delivered to a given material point, the higher its temperature rises, reducing the cooling rate and resulting in a martensite-free microstructure.

From the above calculations, further deductions can be made: the surface energy density („planimetric energy input," e; J/mm^2), volumetric energy density („volumetric energy input," e'; J/mm^3), and unit efficiency (e*; J/mm2 ·√s) can be determined. Surface energy density represents the energy delivered per unit area, while volumetric energy density projects this onto a unit volume. The unit efficiency (bottom part of (Fig. 2), is derived from weighting the formulas for power density and surface energy density, describing the efficiency of energy transfer to the workpiece for a given input power [11].

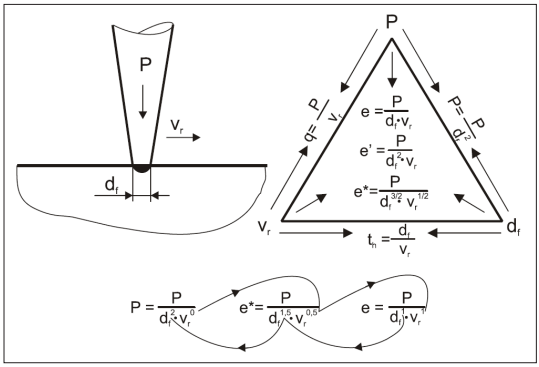

Fig. 2. *Parameter Relationships of High Energy Density Technologies* [11].

2.2.1. Welding Speed with Filler Material

During welding without filler material, the energy of the applied heat source is used to melt the base material. When a filler material is used, additional power is required to melt it [12]:

$$P_{extra} = \dot{m} \cdot \Delta T \cdot c + \dot{m} \cdot L_f \quad (7)$$

where:

$\dot{m}$: wire mass flow rate (g/s),

ΔT: temperature difference between the wire and its melting point (K),

c : specific heat capacity of the filler material (J/(g·K)),

L_f : specific latent heat of melting for steel (J/g)

From this formula, one unknown remains: the wire mass flow rate, which can be calculated as follows [13]:

$$\dot{m} = \rho \cdot A_{huzal} \cdot v_w \quad (8)$$

where:

ρ : density [g/cm^3],

A_{huzal} : wire cross-sectional area [mm^2],

v_w : wire feed speed [mm/s],

Based on this, the additional power requirement can be determined from the energy balance [1], thus the modified welding speed is:

$$v_{új} = v_{alap} \cdot \frac{P_{alap}}{P_{alap} + P_{extra}} \quad (9)$$

2.3. Heat Input

The heat input can also be expressed using the Rosenthal equation and the approach by Bagyinszki and Bitay. The heat input plays a

crucial role in covered arc welding, and the EN 1011-1 standard provides an example for its estimation. A similar formula is applied for laser processing [10]:

$$Q = \frac{\eta \cdot P}{v} \quad (10)$$

where:

η: efficiency (-), which depends on the laser source and the light-matter interaction.

It is worth considering this parameter, as it informs us about the outcome of the processing: high heat input results in slower cooling, leading to a microstructure that does not contain martensite, thereby reducing crack sensitivity. However, if the heat input is excessively high (resulting in very slow cooling), grain coarsening may occur [13]. The ISO 9606-1:2012 standard, according to the International Institute of Welding (IIW), also provides a carbon equivalent calculation to predict crack susceptibility, which determines whether preheating of the workpiece is necessary for a proper weld (CE < 0.4: preheating is not required; above this value, preheating becomes increasingly justified) [3, 9].

2.4. Penetration Depth

The penetration depth in laser welding is typically estimated using the Rosenthal equation. This equation assumes that the weld width is twice the penetration depth, the heat source is point-like, moves at a constant speed across the workpiece, and heat transfer is primarily described by conduction [1]. The equation has both two-dimensional and three-dimensional variants. The 2D model is applicable to cladding welds where penetration depth is negligible [1, 10]. Since we aim to express the penetration depth, the 3D model must be used, which assumes the heat source has a spatial extent and a Gaussian energy distribution:

$$T - T_0 = \frac{q}{2 \cdot \pi \cdot k \cdot h} exp\left(\frac{v_x \cdot \xi}{2 \cdot \kappa}\right) \times K_0\left(\frac{v_x \cdot r}{2 \cdot \kappa}\right) \quad (11)$$

where:

k: thermal conductivity coefficient (W/(m·K)),

h: penetration depth (m),

v_x: heat source velocity in the x-direction (m/s),

ξ: effective distance from the source position in the Lagrange coordinate system (m),

κ: thermal diffusivity coefficient (m^2/s),

K_0: zeroth order of the modified Bessel function (-).

It is worth noting that this equation must be modified when working with materials other than carbon steels or when using a non-continuous laser source [14].

2.5. Shielding Gas Flow

Laser welding falls under the category of fusion welding [3, 9]. Consequently, the molten pool must be protected from the environment (oxidation, contaminants), which is achieved using a shielding gas (or gas mixtures). This medium is directed at the molten pool with a specific flow rate. The gas flow rate (l/min) affects the appearance and, consequently, the mechanical properties of the weld. To ensure a high-quality weld, laminar flow must be maintained, although in some cases, transitional flow conditions may be necessary [10, 14]. This can be demonstrated using the Reynolds number.

$$Re = \frac{\rho \cdot v \cdot d_{spot}}{\mu} \quad (12)$$

where:

Re : Reynolds number (−),

ρ : density of medium (kg/m^3),

v : flow velocity of medium (m/s).

The Reynolds number describes the nature of a medium's (gaseous or liquid) flow, which can be laminar (ordered; Re < 2320), transitional (2320 < Re < 4000), or turbulent (Re > 4000) [15]. In the context of shielding gas flow, this is critical because turbulence can cause gas porosity or uneven protection in the welding zone [3, 9]. During conduction laser welding, laminar flow must be ensured, whereas transitional flow conditions are common in keyhole laser welding [14]. This is due to the specific characteristics of the technology: to allow energy to penetrate deeper layers, the keyhole (as shown on the right side of Fig. 1) must remain open, and the amount of generated plasma and metal vapor must be controlled, as they act as optical media and influence energy transfer [2, 16].

During welding, the desired gas pressure can be set using the shielding gas regulator. However, for professionals, this is not sufficient, as Welding Procedure Specifications (WPS) are typically based on volumetric flow rate:

$$Q = A_{spot} \cdot v = A_{spot} \cdot \frac{Re \cdot \mu}{\rho \cdot d_{spot}} \quad (13)$$

If a flow meter is not incorporated after the regulator, the pressure drop (ΔP) must first be determined using the Bernoulli equation (neglecting changes in elevation) [15]:

$$\Delta P = P_1 - P_2 = \frac{1}{2} \cdot \rho \cdot (v_2^2 - v_1^2) \quad (14)$$

where:

P_1 : pressure (Pa),

P_2 : nozzle exit pressure (Pa),

v_1 : medium velocity at the regulator outlet (m/s),

v_2 : medium velocity at the nozzle exit (m/s).

Based on this, the pressure value to be set on the regulator is the sum of the pressure drop and the nozzle exit pressure. It is important to note that the formula is modified if the nozzle length is not negligibly long [9].

It can be concluded that determining the parameters for laser welding for a specific task is a complex activity. To assist professionals, the calculations discussed earlier also form the basis for simulations [11, 14]. If access to such simulations is not available, it is advisable to conduct a series of experiments with the parameters mentioned in the studies, which can then be optimized for the specific task at hand.

3. Experiment

The key to successful handheld laser welding lies in the careful selection of appropriate technological parameters, which were analyzed in the previous section. The purpose of this chapter is to present the practical experimental investigation conducted at Intertechnika's Csepel workshop using an IPG Photonics LightWeld 1500 XC handheld laser welding device (Fig. 3). This device employs factory-preset welding programs (Fig. 4), ímeaning that precise values of certain input parameters (e.g., power, beam profile) are not accessible. Nevertheless, the focus of our investigation was to determine the extent to which these factory settings ensure high-quality welds.

The equipment used is one of the most advanced handheld laser sources available today [17]. Table. 1 outlines the specifications of the laser source.

Table 1. *IPG Photonics LightWeld 1500 XC machine specifications* [8]

Parameter	Value
Laser power (HPP-pulse mode)	150–2500 W
Laser power (CW-continuous wave mode)	150–1500 W
Operating modes	CW, Track, Modulation, HPP, Stitch, Clean, ADV. Stich
Laser source wavelength	1070 nm
Oscillation frequency	0–300 Hz
Oscillation amplitude	0–15 mm
Input voltage	200–240 V
Current consumption at full load	24 A
Rated power	4600 VA

The system is user-friendly, allowing the selection of a program from a table provided with the machine based on the base material, laser mode, and penetration depth (Fig. 4). Experiments were conducted in continuous wave (CW) mode, both with and without filler material (rows CW and M in the table). For welding with filler material, an IPG LightWELD WF-100 wire feeder device was used.

3.2. Experimental Materials

To investigate different penetration depths, we incrementally increased the sheet thickness from 1 mm to 5 mm in 1 mm steps. Not all sizes were available for a single material type in our environment, so we conducted experiments on DC01 (1 mm and 2 mm) and S355J2 (3 mm and above) carbon steels. In all cases, we produced single-sid-

Fig. 3. *IPG Photonics LightWeld 1500 XC handheld laser source and IPG LightWELD WF-100 wire feeder equipment.*

METAL	SHIELDING GAS	MODE	WELD DEPTH			
			0.040" (1.0mm)	0.080" (2.0mm)	0.120" (3.0mm)	0.160" (4.0mm)
STAINLESS STEEL	NITROGEN	CW	A1	A2	A3	A4
		M	C1	C2	C3	-
		W	A6	A7	A8	A9
MILD STEEL	NITROGEN	CW	E1	E2	E3	E4
		M	F1	F2	F3	-
		W	E6	E7	E8	-
GALVANIZED STEEL	NITROGEN	CW	-	-	-	-
		M	J1	J2	J3	-
		W	-	-	-	-
ALUMINUM 3XXX	ARGON	CW	-	-	-	-
		M	H1	H2	H3	H4
		W	-	-	-	-
ALUMINUM 5XXX	ARGON	CW	-	-	-	-
		M	L1	L2	L3	L4
		W	L6	L7	L8	L9

Fig. 4. *Laser source program table* [8]

ed fillet welds in a T-joint configuration, secured by pre-tacking the sheet ends. We were also interested in the filler material program mode (W: Wire welding), for which we used Böhler EMK 8 Ø1 mm solid wire electrode. As indicated in **Table 2** we consistently used nitrogen with a purity of 4.6 as the shielding gas at an operating pressure of 0.2 MPa.

Table 2. *Composition of the base materials used in the experiment*

Material	C%	Si%	Mn%	P%	S%	Cu%
S355J2	0.2	0.55	1.6	0.025	0.035	0.55
DC01	0.12	-	0.6	0.045	0.045	-
EMK 8	0.11	1	1.8	-	-	-

3.3. Investigation

We aimed to qualify the produced welds, so we conducted penetrant testing and subsequently prepared metallographic specimens for optical examination and hardness testing.

The liquid penetrant testing was performed at the Óbuda University, Bánki Donát Faculty of Mechanical and Safety Engineering. The testing was carried out in accordance with the ISO 3452-1:2021 standard. (**Fig. 5**)

The metallographic examination was conducted at the Budapest facility of Bay Zoltán Applied Research Nonprofit Ltd. The cross-sections to be examined were prepared in accordance with MSZ EN ISO 15614-1:2023. Thinner workpieces were cut using sheet metal shears, while for sheets 4 mm and thicker, an angle grinder was used. This method allowed us to cut a larger area to account for potential heat treatment effects, after which an abrasive cutting machine was employed with water cooling to achieve a size suitable for embedding. Sample preparation was carried out according to MSZ EN ISO 1463:2021. As our focus was solely on examining the weld shapes and potential defects, we polished the samples up to a 1 µm diamond suspension (for macro imaging). To reveal the microstructure, a 5% Nital etchant was used. (**Fig. 6.**)

The hardness testing was conducted within the university premises using the Vickers method with a 200 g load, as the heat-affected zones (HAZ) were expectedly narrow due to the characteristics of the technology. The results showed no anomalies; hardness values increased progressively from the base material toward the weld.

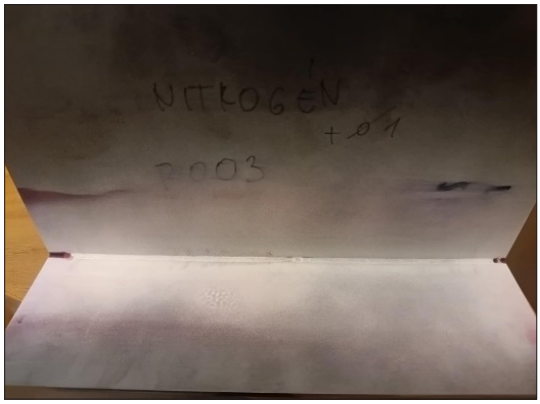

Fig. 5. *Result of penetration testing on a sample welded with filler material using the E8 program on 3 mm thick S355J2 sheet.*

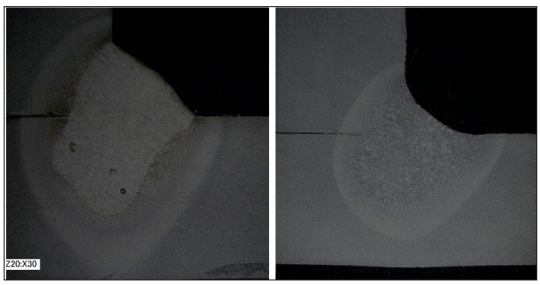

Fig. 6. *Samples made of S355J2 using the E4 program: 5 mm filler material weld (left) and 4 mm base material weld (right).*

3.4. Results

During visual inspection and penetrant testing, no surface-breaking material defects were observed. Microscopic images revealed spherical, porous welds (classified as defect code 2011 according to MSZ EN ISO 6250-1:2008) when using the parameter table recommended by the manufacturer. The most likely cause is uneven beam guidance and uncertainty in maintaining the position of the welding gun.

4. Conclusion

The key to high-quality welding lies in a thorough understanding of the applied technology. In many cases, it is acceptable to rely on seemingly trivial, empirical formulas and guidelines. However, for greater certainty, it is advisable to develop and simulate optimized technological parameters.

One of the sensitive parameters in laser welding is the welding speed, particularly due to the uncertainty associated with manual beam guidance.

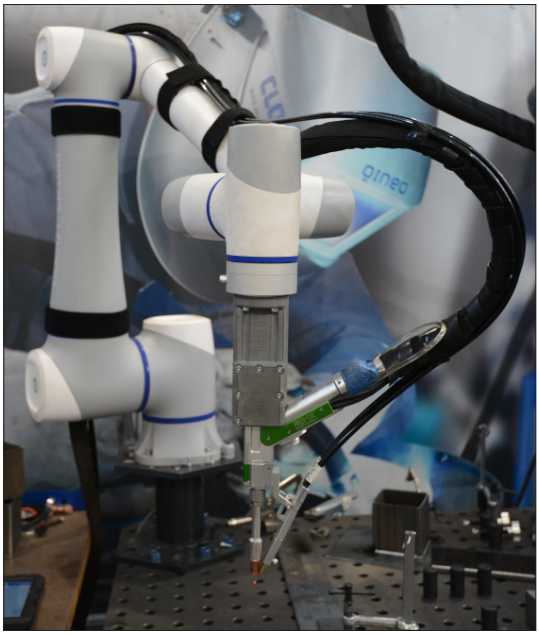

Fig. 7. *FWH20-S10A laser welding gun mounted on CR10A Dobot* **[4]**

Although it involves additional costs (potentially several million forints), creating a Welding Procedure Specification (WPS) for series or mass production is worthwhile, and integrating the laser source with a collaborative robot is recommended **[4]**.

The parameter table shown in **Fig. 4** specifies the shielding gas for welding (nitrogen). Although no evidence was found in the metallographic specimens, it is worth experimenting with other commonly used industrial shielding gases, as nitrogen can form nitrides with alloying elements in the base materials (in our case, potential Mn_4N and Si_3N_4 precipitations could have occurred).

Acknowledgment

The authors would like to express their gratitude to Intertechnika Ltd. for their support in conducting the experimental welds and providing equipment data, and to Bay Zoltán Applied Research Nonprofit Ltd. for their assistance in metallographic sample preparation and microscopic imaging.

References

[1] E. Kannatey-Asibu Jr.: *Principles of Laser Materials Processing Developments and Applications*. 2nd edition, Wiley, Hoboken, NJ, 2023.

[2] Buza G.: *Lézersugaras Technológiák I.* Edutus Főiskola, Budapest, 2012.

[3] Gáti J. (szerk.): *Hegesztési Zsebkönyv I.* Cokom Mérnökiroda Kft., Budapest, 2023.

[4] Gáti J., Kovács T., Nagy B.: *Gépesített kézi lézeres hegesztés gyakorlati tapasztalatai.* Hegesztéstechnika, XXXIV/ 4. (2024) 43–47.

[5] General Electric Company. Industrial hand held laser tool and laser system (US4564736A), Amerikai Szabadalmi Hivatal 1986. https://patents.google.com/patent/US4564736A/en

[6] Halász G.: *Kézi lézeres berendezések biztonságos használata.* Hegesztéstechnika XXXV/1. (2024) 41–47.

[7] MSZ EN ISO 4063:2023: Hegesztés, forrasztás és termikus vágás. A hegesztési eljárások megnevezése és azonosító számuk.

[8] LightWELD® Sorozatú Kézi Lézerhegesztő Rendszer Eredeti Használati Útmutató Fordítása, dokumentumszám: DOCCHUGMPSHU0018, Rev:2 (2023. november 29.)

[9] Bagyinszki G., Bitay E.: *Hegesztéstechnika I.: Eljárások és Gépesítés*. Erdélyi Múzeum-Egyesület, Kolozsvár, 2010. https://doi.org/10.36242/mtf-08

[10] Volpp J.: *High-Power Laser Material Processing for Engineers*. Taylor & Francis Group, LLC, 2025.

[11] Bitay E.: *Lézeres felületkezelés és modellezés*. Erdélyi Múzeum-Egyesület, Kolozsvár, 2007. https://doi.org/10.36242/mtf-04

[12] Salminen Antti Sakari: *Effect of welding parameters on the efficiency and energy distribution during laser welding with filler wire*. ICALEO 2001, Laser Institute of America, 2001. 409–418. https://doi.org/10.2351/1.5059891

[13] Messler, R. W.: *Principles of Welding: Processes, Physics, Chemistry, and Metallurgy*. Wiley, 2004. 167–168.

[14] Hekmatjou H., Zeng Z., Shen J., Oliveira J. P. Naffakh-Moosavy H.: *A comparative study of analytical Rosenthal, finite element, and experimental approaches in laser welding of AA5456 alloy*. Metals, 10/4. (2020) 436. https://doi.org/10.3390/met10040436

[15] Lajos T.: *Az áramlástan alapjai*. 5. kiadás, Akadémiai Kiadó, 2024. https://mersz.hu/lajos-az-aramlastan-alapjai/

[16] Buza G., Erős A., Fazekas É.: *A hegesztési munkagáz összetételének hatása a plazmaképződésre a lézersugaras hegesztés során*. Bányászati és kohászati lapok. Kohászat, 148/6. (2015).

[17] https://spark-co.com/en/2024/05/24/ipg-lightweld-what-you-need-to-know/?utm_source=-chatgpt.com (letöltve: 2025. április 16.)